JPE 3-4-2

New Zero-Current-Transition (ZCT) Circuit Cell Without Additional Current Stress

C.E. Kim, E.S. Choi, and G.W. Moon

Dept. of Electrical Engineering, KAIST, Daejon, Korea

ABSTRACT

In this paper, a new zero-current-transition (ZCT) circuit cell is proposed. The main switch is turned-off under the zero current and zero voltage condition, and there is no additional current stress and voltage stress in the main switch and the main diode, respectively. The auxiliary switch is turned-off under the zero voltage condition, and the main diode is turned-on under the zero voltage condition. The resonant current required to obtain the ZCT condition is relatively small and regenerated to the input voltage source. The operational principles of a boost converter integrated with the proposed ZCT circuit cell are analyzed and verified by the simulation and experimental results.

Keywords: zero-current-transition (ZCT), zero-current-switching (ZCS), zero-voltage-switching (ZVS), power-factor-correction (PFC)

1. Introduction

Nowadays, in order to follow the trend that the electrical systems become compact and light, switched-mode-power-supplies (SMPSs) of those systems must be compact and light. Reactive components, such as transformers, inductors, and capacitors, occupy the considerable volume and weight of SMPSs. Therefore, to minimize the volume and weight of SMPSs, the switching frequency must be increased. However, as the switching frequency increases, the switching losses of semiconductor devices increase in proportion to the switching frequency. As a result, the efficiency of SMPSs decreases, and SMPSs become bulky and heavy due to the heat sinks of semiconductor devices.

To reduce the switching loss, quasi-resonant converters are reported such as zero-voltage-switching (ZVS) and zero-current-switching (ZCS) techniques[1]. But, since voltage stress and current stress of semiconductor devices are increased by the resonance, the conduction losses are increased. In addition, it is difficult to design and control SMPSs because these techniques operate in the variable frequencies.

To overcome these drawbacks, zero-voltage-transition (ZVT) and zero-current transition (ZCT) techniques are proposed[2-14]. These soft switching techniques have the advantages of PWM converters and those of resonant converters. ZVT techniques are suitable for power MOSFETs, because the turn-on switching loss of power MOSFETs is dominant due to the parasitic drain-source capacitance[2-5]. However, for high-power and high-voltage applications, power MOSFETs show the serious problems, that is, the considerable conduction loss due to

This paper was awarded a best papers prize at 2003 Power Electronics Annual Conference.

Corresponding Author: power@angel.kaist.ac.kr Tel: +82-42-869-3475, Fax: +82-42-869-3410

$R_{ds(on)}$ which depends greatly on the voltage rating [6-9].

On the other hand, IGBTs are appropriate for high-power and high-voltage applications because IGBTs have several advantages: the high-power capability, the high-voltage durability, the low conduction loss, and the low cost. But, the fatal disadvantage of IGBTs is the current tail at turn-off and this results in the considerable turn-off switching loss[6, 7, 15, 16]. Therefore, under ZCT condition, the turn-off switching loss can be minimized and the performance of SMPSs can be improved. However, the ZCT circuit cells proposed previously have had some drawbacks. The current stress of the main switch is increased due to the resonant current required to obtain the ZCT condition [10-12]. And the voltage stress of the main diode is increased twice the output voltage[6, 7, 13]. Furthermore, additional components exist in the main power-transfer path[7, 8, 13, 14]. Therefore, the conduction losses are increased and the performance of SMPSs is deteriorated.

In this paper, a new ZCT circuit cell, which does not have the drawbacks mentioned above, is proposed. The main switch is turned-off under the zero current and zero voltage condition, and there is no additional current stress and voltage stress in the main switch. The auxiliary switch is turned-off under the zero voltage condition, and the main diode is turned-on under the zero voltage condition. Furthermore, the peak value of the resonant current required to obtain the ZCT condition is relatively small and regenerated to the input voltage source. The operational principles of a boost converter integrated with the proposed ZCT circuit cell are described. The design guideline and example are presented. The operation of the proposed ZCT circuit cell is verified and the application for the power-factor-correction (PFC) is considered through the simulation and experimental results.

2. Principle of Operation

2.1 New ZCT circuit cell

The proposed ZCT circuit cell is shown in Fig. 1 and consists of the auxiliary switch, Q_A, the resonant capacitor, C_r, the resonant inductor, L_r, and the blocking diode, D_r.

The main features of the proposed ZCT circuit cell are as follows.

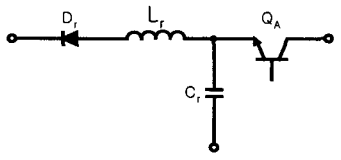

Fig. 1. New ZCT circuit cell.

- The main switch, Q_M is turned-off under zero current condition, the auxiliary switch, Q_A is turned-off under zero voltage condition, and the main diode, D_M is turned-on under zero voltage condition.
- There is no additional current stress and voltage stress at the main switch, Q_M.
- The resonant current required to obtain the ZCT condition is smaller than the peak current of the main inductor and regenerated to the input voltage source.

2.2 Operational Principles of the proposed ZCT boost converter

The circuit diagram of the proposed ZCT boost converter is presented in Fig. 2. To simplify the analysis, the follows are assumed.

- All components are ideal.
- The converter is operating in steady-state.
- The main inductor, L has the large inductance enough to be regarded as the constant current source.
- The output capacitor, C_O has the large capacitance enough to be regarded as the constant voltage source.

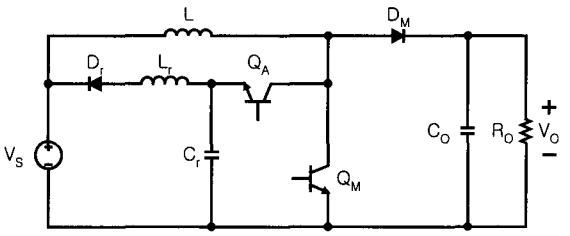

Fig. 2. Circuit Diagram of the proposed ZCT Boost Converter.

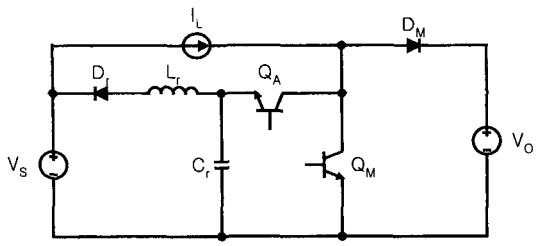

Fig. 3. Equivalent Circuit of the proposed ZCT Boost Converter.

With these assumptions, the equivalent circuit of the proposed ZCT boost converter is shown in Fig. 3. The proposed ZCT boost converter operates in six modes as shown in Fig. 4. And the key waveform of the ZCT boost converter is presented in Fig. 5. Prior to t_0, Q_M and Q_A are turned-off, so all the inductor current, I_L flow into the output voltage source, V_O and the resonant capacitor, C_r is charged $-V_{Cr}$.

i) Mode 1: M_1 (t_0~t_1)

Mode 1 begins as the main switch, Q_M turns on, and the inductor current, I_L flows through Q_M. The ZCT circuit cell does not operate, so the resonant capacitor, C_r holds the initial voltage, $-V_{Cr}$ and no current flows through the resonant capacitor, L_r.

$$i_{Lr}(t) = 0 \tag{1}$$

$$v_{Cr}(t) = -V_{Cr} \tag{2}$$

When Q_A is turned-on, Mode 1 ends.

ii) Mode 2: M_2 (t_1~t_2)

The inductor current, I_L, which flowed through Q_M at Mode 1, flows through the auxiliary switch, Q_A and C_r by the initial voltage of C_r, $-V_{Cr}$ and $v_{Cr}(t)$ increases linearly.

$$i_{Lr}(t) = 0 \tag{3}$$

$$v_{Cr}(t) = \frac{I_L}{C_r}(t - t_1) - V_{Cr} \tag{4}$$

If Q_M is turned-off before $v_{Cr}(t)$ becomes larger than zero, the ZCT of Q_M is obtained. When $v_{Cr}(t)$ reaches V_S, Mode 2 ends.

iii) Mode 3: M_3 (t_2~t_3)

Similarly to Mode 2, the inductor current, I_L flows through Q_A and C_r, and $v_{Cr}(t)$ increases. The voltage of C_r is regenerated to the input voltage source, V_S through L_r and the blocking diode, D_r, because $v_{Cr}(t)$ is larger than V_S.

$$i_{Lr}(t) = I_L\{1 - \cos w(t - t_2)\} \tag{5}$$

$$v_{Cr}(t) = V_S + I_L Z_r \sin w(t - t_2) \tag{6}$$

$$, where\ w = 1/\sqrt{L_r C_r}\ \ and\ \ Z_r = \sqrt{L_r / C_r}$$

When $v_{Cr}(t)$ reaches V_O, Mode 3 ends.

iv) Mode 4: M_4 (t_3~t_4)

The inductor current, I_L flows through the output voltage source, V_O. $v_{Cr}(t)$ is clamped to V_O, and $i_{Lr}(t)$ increases linearly by the constant voltage of L_r, (V_O-V_S).

$$i_{Lr}(t) = \frac{V_O - V_S}{L_r}(t - t_3) + i_{Lr}(t_3) \tag{7}$$

$$v_{Cr}(t) = V_O \tag{8}$$

When Q_A is turned-off, Mode 4 ends.

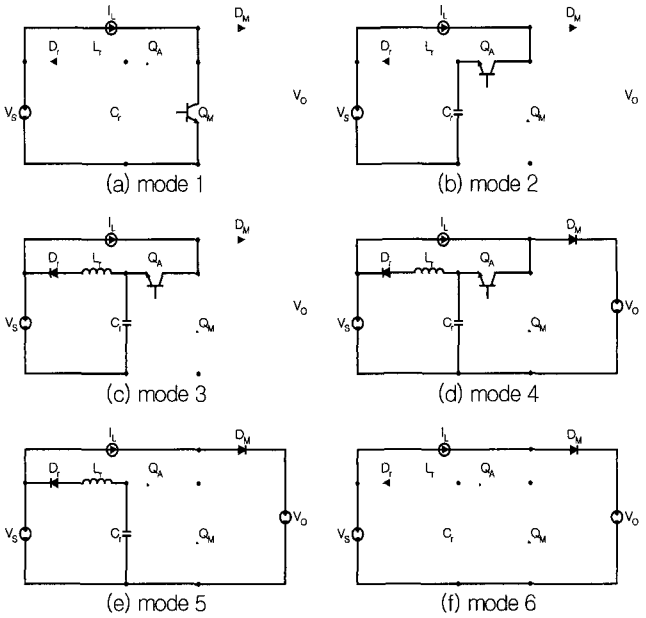

Fig. 4. Operation Modes.

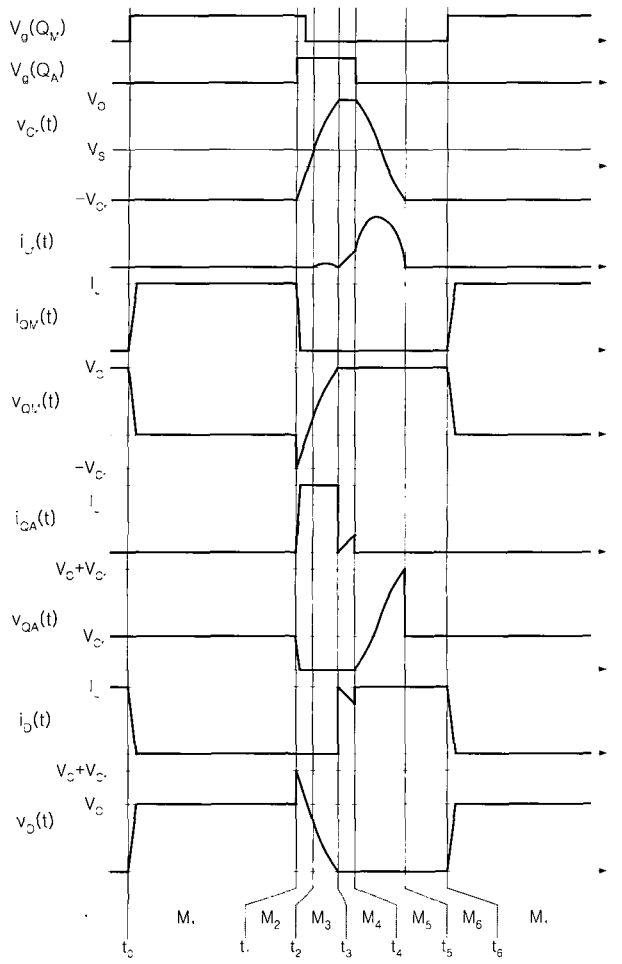

Fig. 5. Key Waveform of ZCT Boost Converter.

v) Mode 5: M_5 (t_4~t_5)

All the inductor current, I_L flow into the output voltage source, V_O. The voltage of C_r and the current of L_r are regenerated to the input voltage source, V_S through L_r and D_r.

$$i_{Lr}(t) = \frac{V_O - V_S}{Z_r}\sin w(t-t_4) + i_{Lr}(t_4)\cos w(t-t_4) \quad (9)$$

$$v_{Cr}(t) = (V_O - V_S)\cos w(t-t_4) - i_{Lr}(t_4)Z_r \sin w(t-t_4) \quad (10)$$

The voltage of C_r is charged to the initial voltage of C_r, $-V_{Cr}$ by the resonance of L_r and C_r.

$$v_{Cr}(t_5) = -V_{Cr} = -\sqrt{(V_O - V_S)^2 + \{i_{Lr}(t_4)Z_r\}^2} + V_S \quad (11)$$

When $i_{Lr}(t)$ reaches 0, Mode 5 ends.

vi) Mode 6: M_6 (t_5~t_6)

All the inductor current, I_L flow into the output voltage source, V_O. The ZCT circuit cell does not operate.

$$i_{Lr}(t) = 0 \quad (12)$$

$$v_{Cr}(t) = -V_{Cr} \quad (13)$$

When Q_M is turned-on, Mode 6 ends.

3. Design Guideline and Example

In this section, the design guideline and example of the proposed ZCT boost converter are given.

The design specification is defined as follows.

- Input voltage: V_S = 50V
- Output voltage: V_O = 200V
- Output power: P_O = 200W
- Predicted efficiency: η = 0.95 (95%)
- Switching Frequency: f_s = 100kHz

i) Calculate I_L at output power, P_O.

$$I_L = \frac{P_O}{V_S \cdot \eta} \quad (14)$$

$$I_L = \frac{200}{50 \times 0.95} = 4.2A$$

ii) Select the desired negative initial voltage of C_r, V_{Cr}.

$$V_{Q_1,\max} = V_O + V_{C_r} \quad (15)$$

$$V_{D_r,\max} = V_S + V_{C_r} \quad (16)$$

$$V_{Q_1,\max} = 200 + V_{C_r} \le 400V$$

$$V_{D_r,\max} = 50 + V_{C_r} \le 200V$$

Select V_{Cr} = 130V.

iii) Calculate the characteristic impedance of L_r and C_r, Z_r required to obtain the selected V_{Cr}. The values of V_{Cr} as a function of Z_r are shown in Fig. 6.

$$V_{Cr} = \sqrt{(V_O - V_S)^2 + \left[Z_r\left\{I_L - \sqrt{I_L^2 - \{(V_O - V_S)/Z_r\}^2}\right\}\right]^2} - V_S \quad (17)$$

Select Z_r = 44.7Ω.

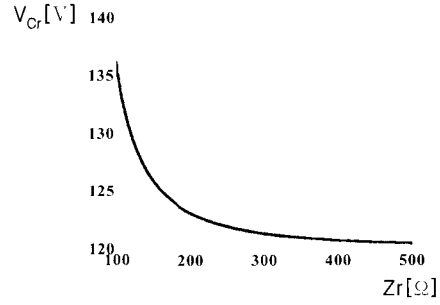

Fig. 6. Values of V_{Cr} as a function of Z_r.

iii) Select the resonant period of L_r and C_r, T_r.

$$0.01T_S \le T_r \le 0.1T_S \tag{18}$$

, *where* T_S *:switching period*, $0.1\mu\text{sec} \le T_r \le 1\mu\text{sec}$

Select $T_r = 1u\text{sec}$.

iv) Calculate the values of L_r and C_r from Z_r and T_r.

$$L_r = \frac{Z_r T_r}{2\pi} \tag{19}$$

$$C_r = \frac{T_r}{2\pi Z_r} \tag{20}$$

$$L_r = 20\mu H, \quad C_r = 10\mu F$$

v) Calculate the duty cycle of the auxiliary switch, d and the time required to obtain the ZCT, T_{ZCT}. The gate signals of the main switch and the auxiliary switch are shown in Fig. 7.

$$d = \frac{1}{T_S}\left\{\frac{C_r}{I_l}(V_S + V_{C_r}) + \sqrt{L_r C_r}\sin^{-1}\left(\frac{V_O - V_S}{Z_r I_L}\right)\right\} \tag{21}$$

$$T_{ZCT} = \frac{C_r}{I_l} V_{C_r} \tag{22}$$

$$d = 0.0343, \quad T_{ZCT} = 0.095u\text{sec}$$

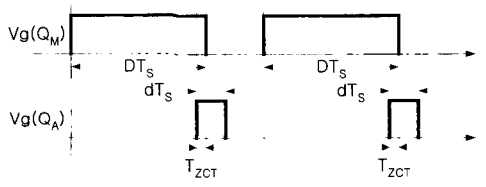

Fig. 7. Gate Signals of Main Switch and Auxiliary Switch.

4. Simulation and Experimental Results

4.1 Experiment 1: Proposed ZCT DC/DC Boost Converter

The prototype of the 200W ZCT boost converter has been implemented to verify the operation and the performance of the proposed ZCT circuit cell. The design specification is presented in Table 1. The circuit used in the experiment 1 is presented in Fig. 8 and the circuit parameters are shown in Table 2. The auxiliary inductor, L_A is added to reduce the resonance of the parasitic inductor and capacitor.

The key waveform of the experiment is shown in Fig. 9, and confirms the operational principles analyzed previously. As shown in the design example, V_{Cr} is 130V. The voltage stress of the auxiliary switch, Q_A is 330V.

Table 1. Design Specification.

V_S	50V	V_O	200V
P_O	200W	f_S	100kHz

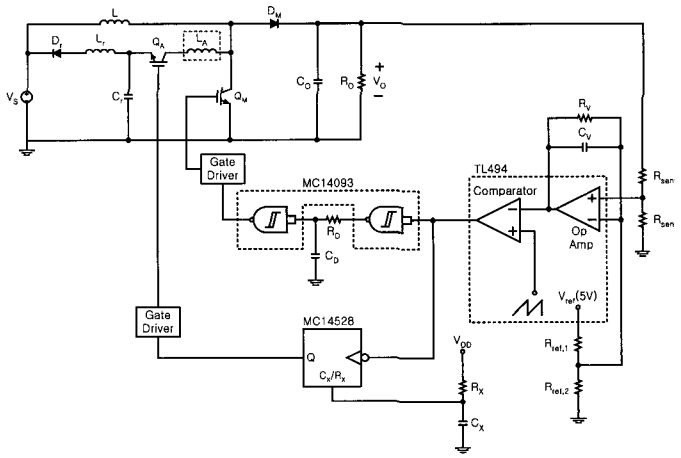

Fig. 8. Circuit used in the Experiment 1.

Table 2. Circuit Parameters.

Q_M	IRG4PC50W (600V, 55A, 2.3V)	C_D	100pF
Q_A	IRG4PC50W (600V, 55A, 2.3V)	C_A	1nF
D_M	15ETH03 (300V, 15A, 40ns)	R_O	200Ω (ELECTRIC LOAD)
D_r	15ETH03 (300V, 15A, 40ns)	R_{sense1}	240kΩ
L	1mH (PQ2625, 41turn)	R_{sense2}	30kΩ
L_r	20uH (PQ2020, 23turn)	R_{ref1}	20kΩ
L_A	4uH	R_{ref2}	20kΩ
C_O	47uF, 250V, 2EA	R_A	100kΩ
C_r	1nF, 630V	R_D	1.3kΩ
C_A	1uF	R_A	270kΩ

The peak current of the main switch, Q_M is 6A, and the peak resonant current is 4A. The voltage peak of D_M is reduced from (V_O+V_{Cr}) to V_O by adding the auxiliary inductor, L_A.

Fig. 10 shows the voltage and current waveforms of the switching device, the main switch, Q_M, the auxiliary switch, Q_A, and the main diode, D_M. Q_M is turned-off under the zero current and zero voltage condition, Q_A is turned-off under the zero voltage condition, and D_M is turned-on under the zero voltage condition. There is no additional current stress and voltage stress at the main switch and the main diode. The waveform of the main switch is presented to compare the proposed converter with the conventional ZCT boost converter[2] in Fig. 11. There is the large resonant current in the conventional ZCT boost converter but there is no resonant current in the proposed converter. Thus, the conduction loss of the proposed converter is smaller than that of the conventional ZCT boost converter.

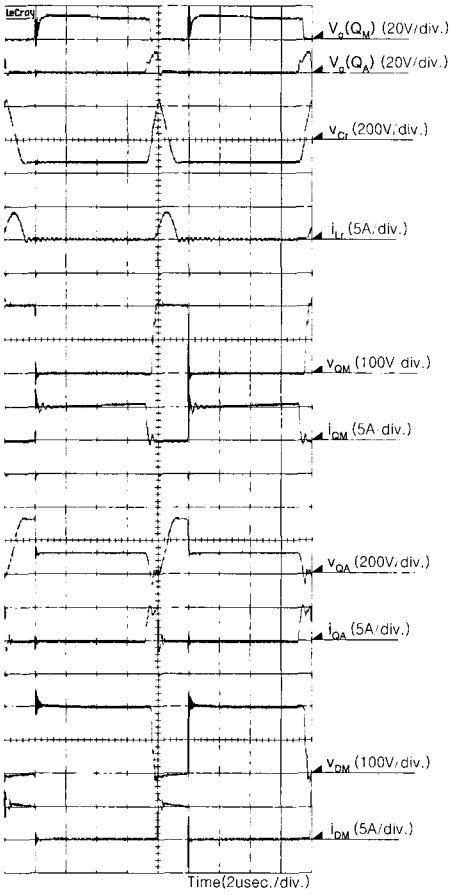

Fig. 9. Key Waveform of Experiment 1.

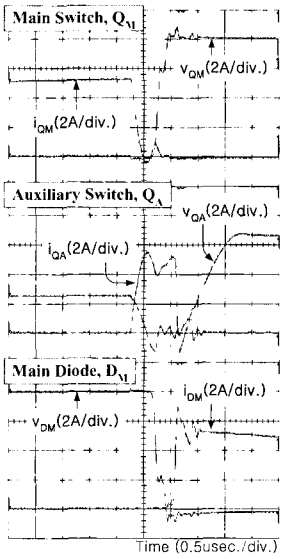

Fig. 10. Zoomed Waveform of Switching Device.

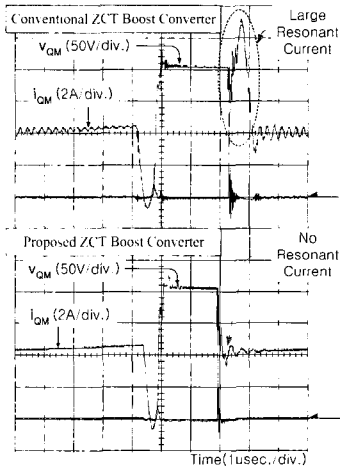

Fig. 11. Comparison with ZCT-PWM Boost Converter.

4.2 Experiment 2: Proposed ZCT AC/DC Boost Converter for PFC Application

The proposed ZCT circuit cell regenerates the power to the input voltage source. Thus, the input current of the ZCT boost converter is discontinuous. But, the regeneration occurs at the short interval of the switching period, the line input current is easily made to be continuous by the line frequency input filter. In this experiment, the proposed ZCT AC/DC boost converter operates in the continuous conduction mode, using the average current mode control to obtain the high power factor. And the power factor correction characteristics are

Table 3. Design Specification.

V_S	85~240V_{AC}	f_S	66kHz
V_O	375V_{DC}	P_O	300W

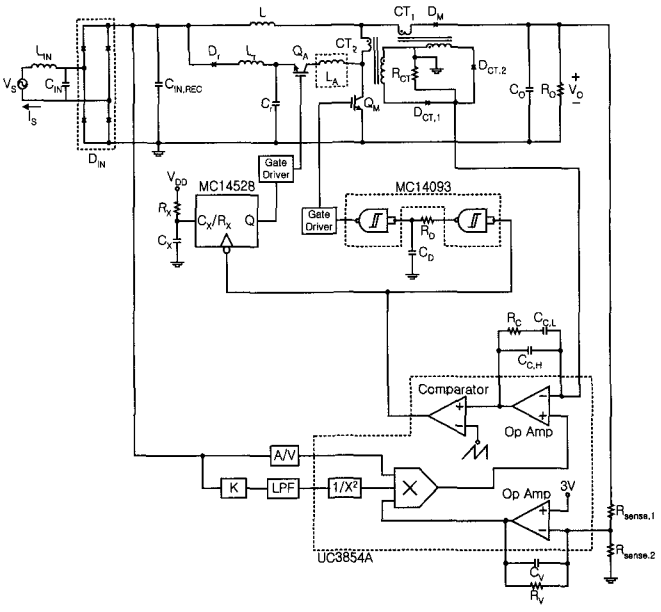

Fig. 12. Circuit used in the Experiment 2.

Table 4. Circuit Parameters.

Q_M	IRG4PC50W (600V, 55A, 2.3V)	$C_{C,L}$	680pF
Q_A	IRG4PF50W (900V, 51A, 2.7V)	$C_{C,H}$	82pF
D_M	10ETF06 (600V, 10A , 50ns)	C_D	470pF
D_{IN}	D15XB60H (600V, 15A)	C_X	1nF
D_r	10ETF06 (600V, 10A , 50ns)	R_O	533.3Ω (ELECTRIC LOAD)
$D_{CT,1}$	11DQ03 (30V, 1.1A, 0.55V_F)	R_{C1}	10Ω
$D_{CT,2}$	11DQ03 (30V, 1.1A, 0.55V_F)	$R_{sense,1}$	1MΩ
L	400uH (PQ3230, 51turn)	$R_{sense,2}$	7.5kΩ
L_{IN}	4.9mH, 3EA	R_V	51kΩ
L_r	20uH (CM234125, 20turn)	R_C	24kΩ
CT_1	$N_P : N_S$ = 1 : 90	R_D	314Ω
CT_2	$N_P : N_S$ = 1 : 90	R_X	1.38kΩ
C_O	220uF, 450V, 3EA	A/V	0.000001
C_{IN}	220nF, 250V_{AC}, 2EA	K	1/51
$C_{IN,REC}$	2.2uF, 630V	LPF	7.2Hz
C_r	10nF	L_A	4uH
C_V	47nF		

shown by the measurement of the power factor and the analysis of the input current harmonics.

The design specification is presented in Table 3. The circuit diagram used in the experiment 2 is presented in Fig. 12 and the circuit parameters are shown in Table 4. The Auxiliary Inductor, L_A is added to reduce the resonance of the parasitic inductor and capacitor in the same manner as the experiment 1.

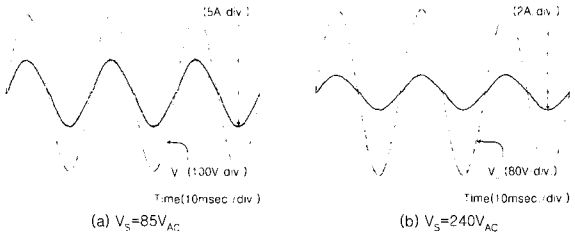

(a) V_S=85V_{AC} (b) V_S=240V_{AC}

Fig. 13. Simulation Waveform of Input Voltage and Input Current.

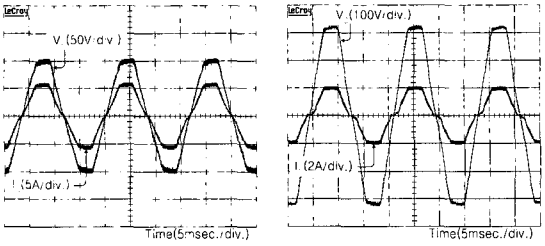

(a) V_S=85V_{AC} (b) V_S=240V_{AC}

Fig. 14. Experimental Waveform of Input Voltage and Input Current.

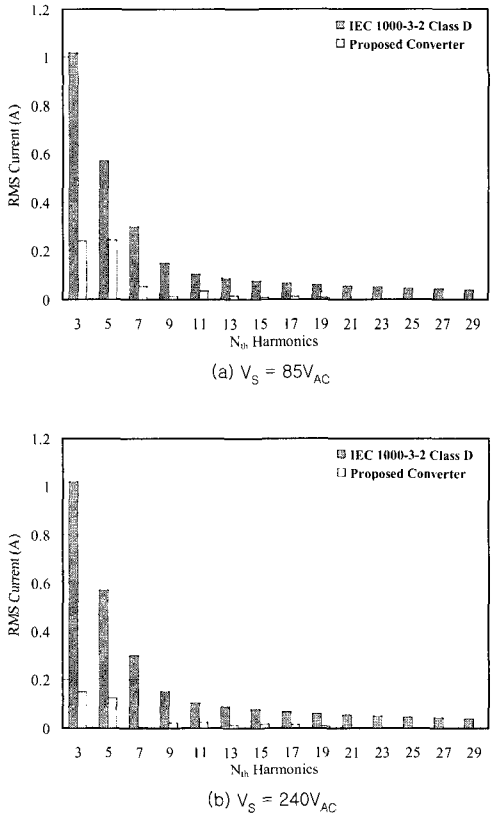

Fig. 15. Harmonics Analysis of Input Current.

The measured power factor from the waveforms presented in Fig. 14 is 0.995 at the minimum input voltage, $85V_{AC}$ and 0.989 at the maximum input voltage, $240V_{AC}$ by the power meter of Voltech Inc., PM3000A. The line harmonic currents of the proposed ZCT AC/DC converter is shown in Fig. 15 (a) and in Fig. 15 (b) at the minimum input voltage, $85V_{AC}$ and the maximum input voltage, $240V_{AC}$, respectively. The proposed ZCT AC/DC converter meets the IEC 1000-3-2 Class D requirement.

5. Conclusions

A new ZCT circuit cell is proposed in this paper. The operational principles of the ZCT boost converter integrated with the proposed ZCT circuit cell are described. The design guideline and example are presented. The operation of proposed ZCT circuit cell is verified through the simulation and experimental results on the 200W prototype of the proposed ZCT DC/DC boost converter. The main switch is turned-off under the zero current and zero voltage conditions, and there is no additional current stress and voltage stress in the main switch. The auxiliary switch is turned-off under the zero voltage condition, and the main diode is turned-on under the zero voltage condition. The peak value of the resonant current required to obtain the ZCT is relatively smaller than the peak current of the main switch, and regenerated to the input voltage source. Furthermore, the application of the PFC is considered through the simulation and experimental results on the 300W prototype of the proposed ZCT AC/DC boost converter.

References

[1] F.C. Lee, "High-frequency quasi-resonant converter technologies," in *Proceedings of the IEEE*, Vol. 76, Issue 4, pp. 377–390, Apr. 1988.

[2] Guichao Hua, Ching-Shan Leu, Yimin Jiang, and F.C. Lee, "Novel zero-voltage-transition PWM converters", *IEEE Transactions on Power Electronics*, Vol. 9, Issue 2, pp. 213–219, March 1994.

[3] Ching-Jung Tseng and Chern-Lin Chen, "Novel ZVT-PWM converters with active snubbers", *IEEE Transactions on Power Electronics*, Vol. 13, Issue 5, pp. 861-869, Sept. 1998.

[4] R. Gurunathan and A.K.S. Bhat, "ZVT boost converter using a ZCS auxiliary circuit", *IEEE Transactions on Aerospace and Electronic Systems*, Vol. 37, Issue 3, pp. 889-897, July 2001.

[5] Chao-Cheng Wu and Chung-Ming Young, "New ZVT-PWM DC/DC converters using active snubber", *IEEE Transactions on Aerospace and Electronic Systems*, Vol. 39, Issue 1, pp. 164-175, Jan. 2003.

[6] R.C. Fuentes and H.L. Hey, "An improved ZCS-PWM commutation cell for IGBT's application", *IEEE Transactions on Power Electronics*, Vol. 14, Issue 5, pp. 939-948, Sept. 1999.

[7] Dong-Yun Lee, Min-Kwang Lee, Dong-Seok Hyun, and I. Choy, "New zero-current-transition PWM DC/DC converters without current stress", *IEEE Transactions on Power Electronics*, Vol. 18, Issue 1, pp. 95-104, Jan. 2003.

[8] C.A. Canesin and I. Barbi, "A novel single-phase ZCS-PWM high-power-factor boost rectifier", *IEEE Transactions on Power Electronics*, Vol. 14, Issue 4, pp. 629-635, July 1999.

[9] Hang-Seok Choi, Bo Hyung Cho, "Novel zero-current-switching (ZCS) PWM switch cell minimizing additional conduction loss", *IEEE Transactions on Industrial Electronics*, Vol. 49, Issue 1, pp. 165–172, Feb. 2002

[10] Guichao Hua, E.X. Yang, Yimin Jiang, and F.C. Lee, "Novel zero-current-transition PWM converters", *IEEE Transactions on Power Electronics*, Vol. 9, Issue 6, pp. 601-606, Nov. 1994.

[11] C.M. de Oliveira Stein and H.L. Hey, "A true ZCZVT commutation cell for PWM converters", *IEEE Transactions on Power Electronics*, Vol. 15, Issue 1, pp. 185-193, Jan. 2000.

[12] Keun-Soo Ma, Gyu-Bum Joung, and Yang-Mo Kim, "New zero-current-switching PWM converters using power MOSFET for lower power applications", in *Proc. IEEE 33rd Power Electronics Specialist Conference*, Vol. 2, pp. 955–960, June 2002.

[13] Hang-Seok Choi and B.H. Cho, "Zero-current-switching (ZCS) power factor pre-regulator (PFP) with reduced conduction losses", in *Proc. IEEE 17th Applied Power Electronics Conference and Exposition*, Vol. 2, pp. 962–967, March 2002.

[14] F.T. Wakabayash, M.J. Bonato, and C.A. Canesin, "Novel high-power-factor ZCS-PWM preregulators", *IEEE Transactions on Industrial Electronics*, Vol. 48,

Issue 2, pp. 322–333, April 2001.

[15] A. Petterteig, J. Lode, and T.M. Undeland, "IGBT turn-off losses for hard switching and with capacitive snubbers", in Proc. IEEE Industry Applications Society, vol. 2, pp. 1501–1507, Sept./Oct. 1991.

[16] V. Venkatesan, M. Eshaghi, R. Borras, and S. Deuty, "IGBT turn-off characteristics explained through measurements and device simulation", in *Proc. IEEE 12th Applied Power Electronics Conference and Exposition,* Vol. 1, pp. 175–178, Feb. 1997.

Chong-Eun Kim was born in Taegu, Korea, in 1978. He received the B.S. degree in the Electrical Engineering from Kyungpook National University, Taegu, Korea, in 2001. In 2003, he received the M.S. degree in the Electrical Engineering from the Korea Advanced Institute of Science and Technology (KAIST), Daejeon, Korea, where he is currently working toward the Ph.D. degree.

His main research interests are DC/DC converters, power-factor-correction (PFC) AC/DC converters, soft switching technique, and digital audio amplifiers.

Eun-Seok Choi was born in Jeonju, Korea, in 1980. In 2002, he received the B.S. degree in the Electrical Engineering from Korea Advanced Institute of Science and Technology (KAIST), Daejeon, Korea, where he is currently working toward the M.S. degree. His main research interests are DC/DC converters, power-factor-correction (PFC) AC/DC converters, and soft switching techniques.

Gun-Woo Moon received the B.S. degree from Han-Yang University, Seoul, Korea, in 1990, and the M.S. and Ph.D. degrees in electrical engineering from the Korea Advanced Institute of Science and Technology (KAIST), Daejeon, Korea, in 1992 and 1996, respectively.

He is currently an assistant professor in the department of electrical engineering and computer science, KAIST. His research interests include modeling, design and control of power converter, soft switching power converter, resonant inverters, distributed power systems, power factor correction, electric drive systems, driver circuit of PDP and flexible AC transmission systems (FACTS). Dr. Moon is a member of KIEE, KIPE, KITE, KIIEIE and IEEE.